Passive Robust Fault Detection for Interval LPV Systems using Zonotopes

Fatiha Nejjari, Saúl Montes de Oca, Vicenç Puig and Atefeh Sadeghzadeh

Automatic Control Department, Universitat Politècnica de Catalunya (UPC), Rambla de Sant Nebridi, 11, 08222 Terrassa, Spain. (e-mail: vicenc.puig@upc.edu).

AbstractIn this paper the problem of robust fault detection using an interval observer for dynamic systems characterized by LPV (Linear Parameter Varying) models is presented. The observer face the robustness problem using two complementary strategies. Parametric modeling uncertainties are considered unknown but bounded by intervals. Their effect is addressed using an interval state observation method based on zonotope representation of the set of possible states. The observer gain is designed via pole placement using LMI (Linear Matrix Inequalities) formulation. The method is applied to a LPV representation of a Twin Rotor MIMO System.

Keywords: Robust Fault Detection, Linear Parameter Varying, Interval LPV Observer, Linear Matrix Inequalities, Zonotopes.

1. INTRODUCTION

Model-based fault detection methods are based on the use of the mathematical models of the monitored system to exploit *analytical redundancy*. Many model-based fault detection techniques, mostly based on linear models, have been investigated and developed in the literature over the last few years. The use of FDI linear-based methods has been extended to non-linear systems using linearization around an operating point (Chen and Patton, 1999). However, for systems with high non-linearity and a wide operating range, the linearized approach fails to give satisfactory results. To tackle this problem new fault detection methods based on non-linear models have been developed. Methods range from the direct use of non-linear models to the use of neural networks, TS fuzzy systems and neuro-fuzzy systems (Chen and Patton, 1999). Alternatively, Linear Parameter Varying (LPV) models have recently attracted the attention of the FDI research community. Such models can be used efficiently to represent some nonlinear systems (Shamma and Cloutier, 1993, Andrés and Balas, 2004). This has motivated some researchers from the FDI community to develop model-based methods using LPV models (see Bokor et al. (2002), among others). But even with the use of LPV models, modeling errors and disturbances are inevitable in complex engineering systems. So, in order to increase reliability and performance of model-based fault detection the development of robust fault detection algorithms should be addressed. The robustness of a fault detection system means that it must be only sensitive to faults, even in the presence of model-reality differences (Chen and Patton, 1999). One of the approaches to robustness, known as *passive*, is based on enhancing the robustness of the fault detection system at the decision-making stage. The aim with the passive approach is usually to determine, given a set of models, if there is a member in the set that can explain the measurements. A common approach to this problem is to propagate the model uncertainty to the alarm limits of the residuals. When the residuals are outside of the alarm limits it is argued that model uncertainty alone can not explain the residual and therefore a fault must have occurred. This approach has the drawback that faults that produce a residual deviation smaller than the residual uncertainty due to parameter uncertainty will not be detected. Another approach to the passive robust fault detection problem is to explicitly calculate the set of states that are consistent with the measurements. When a measurement is found to be inconsistent with this set, a fault is assumed to have occurred. As an exact representation of the set of states consistent with the measurements is hard to calculate, approximating sets that provide outer bounds are often used instead. In the literature several approximating sets to enclose the set of possible states have been proposed. In Witczak et al. (2002), a state estimator based on enclosing the set of states by the smallest ellipsoid is proposed following the algorithms proposed by Maksarov and Norton (1996). However, in this approach only additive uncertainty is considered, but not the multiplicative one introduced by modeling uncertainty located in the parameters. In this paper, both types of uncertainties are considered as in Rinner and U. Weiss (2004), but there only system trajectories obtained from the uncertain parameter interval vertices are considered, assuming that the monotonicity property holds.

The main contribution of this paper is to develop a passive robust fault method for LPV systems that uses a interval observer approach based on enclosing the set of states by zonotopes. The proposed state-estimator applied to fault detection follows a consistency based approach that is based on determining the set of states that are consistent with parameter and measurement uncertainty.

The structure of this paper is organized as follows. The LPV systems that uses a interval LPV observer is introduced in Section 2. Additionally, a solution for the design of an interval LPV observer via pole placement using linear matrix inequality (LMI) formulation is proposed. Section 3 explain the fault detection test using interval LPV observers. In Section 4 the

implementation of interval LPV observers using zonotope approach is presented. Finally in Section 5, an illustrative example based on the Twin-Rotor MIMO System (TRMS) is used to assess the validity of the results derived in the paper.

2. INTERVAL OBSERVERS FOR LPV SYSTEMS

2.1 System set-up

Let us consider that the nonlinear system to be monitored can be described by its LPV representation as follows:

$$\begin{aligned} x(k+1) &= \tilde{A}(\vartheta_k)x(k) + \tilde{B}(\vartheta_k)u(k) \\ y(k) &= \tilde{C}(\vartheta_k)x(k) + \tilde{D}(\vartheta_k)u(k) \end{aligned} \tag{1}$$

where $u(t) \in \Re^{n_u}$ is the system input, $y(t) \in \Re^{n_y}$ is the system output and $x(t) \in \Re^{n_x}$ is the state-space vector. $\vartheta_k := \vartheta(k)$ is a vector of time-varying parameters of dimension n_ϑ that changes with the operating point scheduled by some measured system variables p_k ($p_k := p(k)$) that can be estimated using some known function: $\vartheta_k = f(p_k)$. However, some uncertainty in the estimated parameter values is considered to be bounded by the following set:

$$\Pi_k = \{\vartheta_k \in \Re^{n_\vartheta} \mid \underline{\vartheta_k} \leq \vartheta_k \leq \overline{\vartheta_k}\} \tag{2}$$

This set represents the uncertainty about the exact knowledge of real system parameters ϑ_k. The interval for uncertain parameters can be inferred from real data using set-membership parameter estimation algorithms (Milanese et al., 1996).

System (1) describes a model parametrized by a scheduling variable denoted by p_k. In this paper, the kind of LPV system considered are those whose parameters vary affinely in a polytope (Apkarian et al., 1995). In particular the state-space matrices range in a polytope of matrices defined as the convex hull of a finite number, N, of matrices. That is,

$$\begin{aligned} \begin{pmatrix} \widetilde{A}(\vartheta_k) & \widetilde{B}(\vartheta_k) \\ \widetilde{C}(\vartheta_k) & \widetilde{D}(\vartheta_k) \end{pmatrix} &\in Co\left\{ \begin{pmatrix} A_j(\vartheta^j) & B_j(\vartheta^j) \\ C_j(\vartheta^j) & D_j(\vartheta^j) \end{pmatrix}, \right\} \\ &:= \sum_{j=1}^{N} \alpha^j(p_k) \begin{pmatrix} A_j(\vartheta^j) & B_j(\vartheta^j) \\ C_j(\vartheta^j) & D_j(\vartheta^j) \end{pmatrix}, \end{aligned} \tag{3}$$

with $\alpha^j(p_k) \geq 0$, $\sum_{j=1}^{N} \alpha^j(p_k) = 1$ and $\vartheta^j = f(p^j)$ is the vector of uncertain parameters of j^{th} model where each j^{th} model is called vertex system and it is assumed according to property (2) that: $\vartheta^j \in [\underline{\vartheta^j},\ \overline{\vartheta^j}]$.

Consequently, the LPV system (1) can be expressed as follows:

$$\begin{aligned} x(k+1) &= \sum_{j=1}^{N} \alpha^j(p_k) \left[A_j(\vartheta^j)x(k) + B_j(\vartheta^j)u(k)\right] \\ y(k) &= \sum_{j=1}^{N} \alpha^j(p_k) \left[C_j(\vartheta^j)x(k) + D_j(\vartheta^j)u(k)\right] \end{aligned} \tag{4}$$

Here A_j, B_j, C_j and D_j are the state space matrices defined for j^{th} model. Notice that, the state space matrices of system (1) is equivalent to the interpolation between LTI models, for example: $\tilde{A}(\vartheta_k) = \sum_{j=1}^{N} \alpha^j(p_k) A_j(\vartheta^j)$.

The polytopic system is scheduled through functions $\alpha^j(p_k), \forall j \in [1, \ldots, N]$ that lie in a convex set:

$$\Psi = \Big\{ \alpha^j(p_k) \in \Re^N, \alpha(p_k) = \left[\alpha^1(p_k), \ldots, \alpha^N(p_k)\right]^T, \\ \alpha^j(p_k) \geq 0,\ \forall j,\ \sum_{j=1}^{N} \alpha^j(p_k) = 1 \Big\}. \tag{5}$$

There are several ways of implementing (3) depending on how $\alpha^j(p_k)$ functions are defined (Murray-Smith and Johansen, 1997). Here the approach used in Baranyi et al. (2003) is proposed:

$$\begin{aligned} &\begin{pmatrix} \widetilde{A}(\vartheta_k) & \widetilde{B}(\vartheta_k) \\ \widetilde{C}(\vartheta_k) & \widetilde{D}(\vartheta_k) \end{pmatrix} \\ &= \sum_{j=1}^{N} \underbrace{\sum_{i_1=1}^{2} \cdots \sum_{i_v=1}^{2} \prod_{m=1}^{v} \mu_{m,i_m}(p_m(k))}_{\alpha^j(p_k)} \begin{pmatrix} A_j(\vartheta^j) & B_j(\vartheta^j) \\ C_j(\vartheta^j) & D_j(\vartheta^j) \end{pmatrix} \end{aligned} \tag{6}$$

with $\mu_{m,1} = \dfrac{\left(p_m(k) - \underline{p_m^j}\right)}{\left(\overline{p_m^j} - \underline{p_m^j}\right)}$ and $\mu_{m,2} = 1 - \mu_{m,1}$ where $\overline{p_m^j}$ and $\underline{p_m^j}$ represent the upper and lower bounds of p_m respectively and v is the number of scheduling variables.

2.2 Interval observer

The system described by (1) is monitored using a linear observer with Luenberger structure considering parameter uncertainty given by $\vartheta^j \in [\underline{\vartheta^j},\ \overline{\vartheta^j}]$. In the following, we consider only strictly proper systems such that $D = 0$. Consequently, the interval LPV observer can be written as:

$$\begin{aligned} \hat{x}(k+1) &= \sum_{j=1}^{N} \alpha^j(p_k) \left[A_{0,j}(\vartheta^j)\hat{x}(k) + B_j(\vartheta^j)u(k) + L_j y(k)\right] \\ \hat{y}(k) &= \sum_{j=1}^{N} \alpha^j(p_k) \left[C_j(\vartheta^j)\hat{x}(k)\right] \end{aligned} \tag{7}$$

where $A_{0,j}(\vartheta^j) = A_j(\vartheta^j) - L_j C_j(\vartheta^j)$, $u(k)$ is the measured system input vector, $\hat{x}(k)$ is the estimated system state vector, $\hat{y}(k)$ is the estimated system output vector and L_j is the observer gain that has to be designed in order to stabilize the observer given by (7) for all $\vartheta^j \in [\underline{\vartheta}^j, \overline{\vartheta}^j]$.

Definition 1. *Consider the state estimator given by (7), an initial compact set $\mathbb{X}_0$ and a sequence of measured inputs $(u_i)_0^{k-1}$ and outputs $(y_i)_0^{k-1}$. The* ***exact uncertain estimated state set*** *at time k is expressed by*

$$\begin{aligned} \mathbb{X}_k = \Big\{ \hat{x}_k :\ & (\hat{x}_i = \tilde{A}(\vartheta_{i-1})\hat{x}_{i-1} + \tilde{B}(\vartheta_{i-1})u_{i-1} \\ & + \tilde{L}(y_{i-1} - \hat{y}_{i-1}))_{i=1}^{k}, (\hat{y}_{i-1} = \tilde{C}(\vartheta_{k-1})\hat{x}_{i-1})_{i=1}^{k} \\ & \mid \quad \hat{x}_0 \in \mathbb{X}_0, \quad (\vartheta_{i-1} \in \Pi_i)_{i=1}^{k} \Big\} \end{aligned} \tag{8}$$

where $\tilde{L} = \sum_{j=1}^{N} \alpha^j(p_k) L_j$.

The uncertain state set described in *Definition 1* at time k can be computed approximately by admitting the rupture of the existing relations between variables of consecutive time instants. [1] This makes possible to compute an approximation of this set from the approximate uncertain state set at time *k*-1.

Definition 2. *Consider the state estimator given by (7), the set of uncertain states at time k-1, $\mathbb{X}_{k-1}$ and the input/ouput values (u_{k-1}, y_{k-1}). Then, the set of estimated states at time k based on the measurements up to time k-1 is defined as:*

[1] However, the problem of uncertainty propagation (wrapping effect) could appear when this set is approximated in this way because of the accumulation of overestimation along the time and deriving in an explosion of uncertainty.

$$\mathbb{X}_k^e = \Big\{ \hat{x}_k : \tilde{A}(\vartheta_{k-1})\hat{x}_{k-1} + \tilde{B}(\vartheta_{k-1})u_{k-1} + \tilde{L}(y_{k-1} - \hat{y}_{k-1}), \quad \hat{y}_{k-1} = \tilde{C}(\vartheta_{k-1})\hat{x}_{k-1} \mid \hat{x}_{k-1} \in \mathbb{X}_{k-1}, \vartheta_{k-1} \in \Theta_k \} \tag{9}$$

Analogously, considering measurement equation in (7), the approximated set of estimated outputs $\mathbb{Y}_k^e$ can be determined.

Since the set of estimated states $\mathbb{X}_k^e$ is difficult to compute, one way is to bound it using some geometric regions easy to compute as for example: a box (interval hull) as in Puig et al. (2002), an ellipsoid as in Maksarov and Norton (1996) or a zonotope as in Alamo et al. (2005).

Here, the set of estimated states $\mathbb{X}_k^e$ (or outputs $\mathbb{Y}_k^e$) introduced in *Definition 2* will be approximated iteratively using zonotopes. From these zonotopes, an interval for each state variable can also be obtained by computing the interval hull of the zonotope. The sequence of interval hulls $\square\mathbb{X}_k^e$ with $k \in [0, N]$ will be called the ***interval LPV observer estimation*** of the system given by (7). Analogously, the sequence of interval hulls $\square\mathbb{Y}_k^e$ can be obtained. Following the previous idea, *Algorithm 1* is proposed to determine an approximation of ***set of uncertain estimated states***.

Algorithm 1 Interval LPV Observer using Set Computations

1: $k \leftarrow 1$
2: **while** $k \leq N$ **do**
3: Obtain and store input-output data $\{u_{k-1}, y_{k-1}\}$
4: Compute the approximated set of estimated outputs, $\mathbb{Y}_k^e$
5: Compute the interval hull of the approximated set of estimated outputs, $\square\mathbb{Y}_k^e = \left[\underline{y}_k, \overline{y}_k\right]$
6: $k \leftarrow k + 1$
7: **end while**

2.3 Observer design

The design of the interval LPV observer (7) can be solved with the LMI pole placement technique (Chilali and Gahinet, 1996), that allows to locate the poles of the observer in a subregion of the left half-plane using a LMI region.

Consider a given $2d \times 2d$ Hermitian matrix defined as

$$R = \begin{bmatrix} R_{00} & R_{10} \\ R_{10}^* & R_{11} \end{bmatrix} \in \mathbb{C}^{2d\times 2d}, R_{11} \in \mathbb{C}^{d\times d} \geq 0 \tag{10}$$

and the feasibility set of an associated LMI defined as

$$\mathcal{D} = \Big\{ s \in \mathbb{C} : R_{00} + (R_{10}s)^H + R_{11}s^*s < 0 \Big\} \tag{11}$$

where $(R_{10}s)^H$ denotes the Hermitian transpose of $R_{10}s$. Sets defined according (10)-(11) are called $\mathcal{D}$-regions (Chilali and Gahinet, 1996). Moreover, the intersection of $\mathcal{D}$-regions is a $\mathcal{D}$-region, allowing to characterize some multiple temporal specifications. For example, for the vertical left half-plane characterized by $x < \lambda$, the associated matrix R is

$$R = \begin{bmatrix} -2\lambda & 1 \\ 1 & 0 \end{bmatrix} \tag{12}$$

while for an open disk with center $c = c_1 + c_2 i$ and radius r is

$$R = \begin{bmatrix} c_1^2 + c_2^2 - r^2 & -c_1 + c_2 i \\ -c_1 - c_2 i & 1 \end{bmatrix} \tag{13}$$

Using these formulas, it is easy to verify that the classical stability regions for continuous-time (left half-plane) and discrete-time (origin-centered unitary disk) systems are associated to the matrices

$$R_{ct} = \begin{bmatrix} 0 & 1 \\ 1 & 0 \end{bmatrix}, \quad R_{dt} = \begin{bmatrix} -1 & 0 \\ 0 & 1 \end{bmatrix} \tag{14}$$

In particular, let consider a disk LMI region called $\mathcal{D}$ defined by center c (in this case $c = c_1$ and $c_2 = 0$) and a radius r such that $(c + r) < 1$. The two scalars c and r are used to determine a specific region included in the unit circle where the observer eigenvalues will be placed. Therefore, this circular region puts a lower bound on both the exponential decay rate and the damping ratio of the closed-loop response. The design of the interval LPV observer (7) such that the observer poles are placed in this LMI region requires to find for each vertex j^{th} (with $j \in [1, \ldots, N]$) the observer gain L_j and unknown symmetric matrix $X_j = X_j^T > 0$ thats satisfies the following LMI:

$$\begin{pmatrix} -rX_j & cX_j + (A_{0,j}(\vartheta^j)^T X_j)^T \\ (c + A_{0,j}(\vartheta^j)^T)X_j & -rX_j \end{pmatrix} < 0, \tag{15}$$

for $\vartheta^j \in [\underline{\vartheta^j}, \overline{\vartheta^j}]$, that corresponds to Eq. (10) in Chilali and Gahinet (1996) with matrix A being transpose of the observer matrix $A_{0,j}$.

Note that expression (15) is a Bilinear Matrix Inequality (BMI) which cannot be solved with LMI classical tools. But substituting $W_j = L_j^T X_j$ it is possible to transform it into:

$$\begin{bmatrix} -rX_j & \cdots \\ (c + A_j(\vartheta^j)^T)X_j - C_j(\vartheta^j)^T W_j & \cdots \\ cX_j + X_j^T A_j(\vartheta^j) - W_j^T C_j(\vartheta^j) & -rX_j \end{bmatrix} < 0. \tag{16}$$

Then, the design procedure boils down to solving the LMI (16) and then determining $L_j = (W_j X_j^{-1})^T$. Finally, the observer gains L_j will be interpolated to obtain the interval LPV observer (7).

3. FAULT DETECTION USING LPV OBSERVERS

3.1 Input-output form

The system (1) can be expressed in input-output form using the shift operator q^{-1} and assuming zero initial conditions as follows:

$$y(k) = G_u(q^{-1}, \vartheta_k)u(k) \tag{17}$$

where:

$$G_u(q^{-1}, \vartheta_k) = C(\vartheta_k)(qI - A(\vartheta_k))^{-1}B(\vartheta_k) + D(\vartheta_k) \tag{18}$$

The effect of the uncertain parameters ϑ_k on the observer temporal response $\hat{y}(k, \vartheta_k)$ will be bounded using an interval satisfying [2]:

$$\hat{y}(k) \in \left[\underline{\hat{y}}(k), \overline{\hat{y}}(k)\right] \tag{19}$$

in a non-faulty case.

The application of observers to fault detection consists in testing whether the measured output is consistent with the one given by an observer using a faultless model. If an inconsistency is detected, the existence of a fault is proved. In case of modeling a dynamic system using an interval model, the

[2] In the remainder of the paper, interval bounds for vector variables should be considered component wise.

predicted output is described by a set that can be bounded using an interval. Then, the fault detection test can be stated as:

$$y(k) \notin \square\mathbb{Y}_k^e \tag{20}$$

where $\mathbb{Y}_k^e$ is the set of predicted outputs that can be obtained using *Algorithm 1* and $\square\mathbb{Y}_k^e = [\underline{y}_1, \overline{y}_1] \times \cdots \times [\underline{y}_{n_y}, \overline{y}_{n_y}]$.

Algorithm 2 implements fault detection using interval LPV observers and the fault detection test presented in (20).

Algorithm 2 Fault Detection using Interval LPV Observers

1: $fault \leftarrow FALSE$
2: $k \leftarrow 0$
3: $\mathbb{X}_k^e \Leftarrow \mathbb{X}_0$
4: **while** $fault = FALSE$ **do**
5: Obtain input-output data $\{u_k, y_k\}$
6: Compute the set of estimated outputs, $\mathbb{Y}_k^e$ using *Algorithm 1*
7: **if** $y(k) \notin \square\mathbb{Y}_k^e$ **then**
8: $fault \leftarrow TRUE$ (Fault detection test (20))
9: **end if**
10: $k \leftarrow k + 1$
11: **end while**

3.2 Residual form

Alternatively, a fault detection based on generating a residual can be used. The residual is generated by comparing the measurements of physical variables $y(t)$ of the process with their estimation $\hat{y}(k)$ provided by the associated system model:

$$r(k) = y(k) - \hat{y}(k) \tag{21}$$

where $r(k) \in \Re^{n_y}$ is the residual set and $\hat{y}(k)$ is the prediction obtained using the nominal LPV model.

When considering model uncertainty located in parameters, the residual generated by (21) will not be zero, even in a non-faulty scenario. To cope with the parameter uncertainty effect a passive robust approach based on adaptive thresholding can be used (Horak, 1988). Thus, using this passive approach, the effect of parameter uncertainty in the residual $r(k)$ (associated to each system output $y(k)$) is bounded by the interval:

$$r(k) \in [\underline{r}(k), \overline{r}(k)] \tag{22}$$

where:

$$\underline{r}(k) = \underline{\hat{y}}(k) - \hat{y}(k) \text{ and } \overline{r}(k) = \overline{\hat{y}}(k) - \hat{y}(k) \tag{23}$$

being $\underline{\hat{y}}(k)$ and $\overline{\hat{y}}(k)$ the bounds of the predicted output (19) that can be obtained using observer (7), *Algorithm 1* and $\square\mathbb{Y}_k^e = [\underline{y}_1, \overline{y}_1] \times \cdots \times [\underline{y}_{n_y}, \overline{y}_{n_y}]$.

Then, a fault is indicated if the residuals do not satisfy the relation given by (22). Note that the fault detection test in *Algorithm 2* can be implemented using (22), instead of using (20).

4. IMPLEMENTATION USING ZONOTOPES

4.1 Introduction

In this paper, zonotopes are used to bound the set of uncertain estimated sets. Let us introduce zonotopes.

Definition 3. *The Minkowski sum of two sets* $\mathbb{X}$ *and* $\mathbb{Y}$ *is defined by* $\mathbb{X} \oplus \mathbb{Y} = \{x + y : x \in \mathbb{X}, y \in \mathbb{Y}\}$.

Definition 4. *Given a center vector* $\pi \in \Re^n$ *and a matrix* H $\in \Re^{n \times m}$ *the Minkowski sum of the segments defined by the columns of matrix* H*, is called a* ***zonotope*** *of order m (see Fig. 1). This set is represented as:*

$$\mathbb{X} = \pi \oplus H\beta^m = \{\pi + Hz : z \in \beta^m\}$$

where: β^m *is a unitary box, composed by* m *unitary intervals.*

Then, a zonotope $\mathbb{X}$ of order *m* can be viewed as the Minkowski sum of m segments. The order m is a measure for the geometrical complexity of the zonotopes.

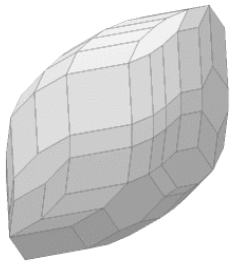

Figure 1. Zonotope of order m=14

Definition 5. *The* ***interval hull*** $\square\mathbb{X}$ *of a closed set* $\mathbb{X}$ *is the smallest interval box that contains* $\mathbb{X}$.

Given a zonotope $\mathbb{X} = \pi \oplus H\beta^m$, its interval hull can be easily computed by evaluating $\pi \oplus H\beta^m$, for all $i = 1..n$: $\square\mathbb{X} = \{x : |x_i - \pi_i| \leq \|H_i\|_1\}$ where H_i is i^{th}-row of H, and x_i and π_i are i^{th} components of x and π, respectively.

4.2 Implementation of interval LPV observers using zonotopes

To implement interval LPV observers using zonotopes, it should be noticed that using (7) as the expression of the estimator model, it can be viewed as a discrete-time system with one input that can be reorganized as:

$$\hat{\mathbf{x}}_{k+1} = A_o(\vartheta_k)\hat{x}_k + B_o(\vartheta_k)u_k^o \tag{24}$$

where:
$A_o(\vartheta_k) = \tilde{A}(\vartheta_k) - \tilde{L}\tilde{C}(\vartheta_k)$, $B_o(\vartheta_k) = \left[\, \tilde{B}(\vartheta_k) \;\; 0 \;\; \tilde{L} \,\right]$ and $u_k^0 = \left[\, u_k \;\; y_{k+1} \;\; y_k \,\right]^T$.

Then, the problem of interval observation can be formulated as a problem of interval simulation and requires characterizing the set $\mathbb{X}_k^e$. This set can be viewed as the ***direct image*** evaluation of (24) and can be implemented using zonotopes.

According to *Algorithm 1*, interval LPV observers involves a bounding operation applied to the set of estimated states $\mathbb{X}_k^e$.

4.3 Implementation of prediction set step

The prediction set step requires characterizing the set $\mathbb{X}_k^e$. This set can be viewed as the ***direct image*** evaluation of $f(x_k, \vartheta_k) = A_o(\vartheta_k)\hat{x}_k + B_o(\vartheta_k)u_k^o$. There are different algorithms to bound such an image using ellipsoids (see Maksarov and Norton (1996)) or zonotopes (see Kuhn (1998)). To bound such image using zonotopes the following result is used:

Theorem 1. *"Zonotope Inclusion" (see Alamo et al. (2005)). Consider a family of zonotopes represented by* $\mathbb{X} = \pi \oplus M\beta^m$

where $\pi \in \Re^n$ is a real vector and $M \in \mathbb{I}^{n\times m}$ is an interval matrix. A zonotope inclusion $\diamond(\mathbb{X})$ is defined by:

$$\diamond(\mathbb{X}) = \pi \oplus [\text{mid}(M \;\; G)] \begin{bmatrix} \beta^m \\ \beta^n \end{bmatrix} = \pi \oplus J\beta^{n+m}$$

where $G \in \Re^{n\times n}$ is a diagonal matrix that satisfies: $G_{ii} = \sum_{j=1}^{m} \frac{\text{diam}(M_{ij})}{2}, i = 1, 2 \ldots n$. with mid *denotes the center and* diam *the diameter of the interval according to Moore (1966). Under this definition, $\mathbb{X} \subseteq \diamond(\mathbb{X})$.*

This prediction step aims at computing the zonotope $\mathbb{X}^e_{k+1}$ that bounds the trajectory of the system at instant *k+1*, from the previous approximating zonotope at time instant *k*, $\mathbb{X}_k$, using the natural interval extension of (24) as suggested by Moore (1966) and the zonotope inclusion operator, as a generalization of Kühn's method (see Kuhn (1998)):

$$\mathbb{X}^e_{k+1} = \pi_{k+1} \oplus H_{k+1}\beta^r \tag{25}$$

where:

$$\pi_{k+1} = \text{mid}(A_o(\vartheta_k))\pi_k + \text{mid}(B_o(\vartheta_k))u^o_k$$

and

$$H_{k+1} = [J_1 \;\; J_2 \;\; J_3]$$
$$J_1 = \diamond(A_o(\vartheta_k)H_k)$$
$$J_2 = \pi_k \left(\frac{\text{diam}(A_o(\vartheta_k))}{2}\right)$$
$$J_3 = u^o_k \left(\frac{\text{diam}(B_o(\vartheta_k))}{2}\right)$$

J_1 is calculated using the zonotope inclusion operator.

It is important to notice that the set of estimated states has an increasing number of segments generating the zonotope $\mathbb{X}^e_{k+1}$ using this method. In order to control the domain complexity, a reduction step is thus implemented. Here we use the method proposed in Combastel (2003) to reduce the zonotope complexity.

4.4 Checking for intersection emptiness

The step 7 of *Algorithm 2* requires to check if the intersection of $[y_k] \cap \mathbb{Y}^e_k$, is not the empty set, before introducing such operation, an additional definition is introduced.

Definition 6. Given the zonotope $\mathbb{Y}^e_k = \pi \oplus H\beta^r$, the strip $[y_k] = \{x \in \Re^n | c^T x\text{-}d| \leq \sigma\}$, a hyperplane $S = \{x : c^T x = q\}$ is a supporting hyperplane of a zonotope $\mathbb{Y}^e_k$ if either $c^T x \leq q, \forall x \in \mathbb{Y}^e_k$ or else $c^T x \geq q, \forall x \in \mathbb{Y}^e_k$ with equality occurring for some $x \in \mathbb{Y}^e_k$. The two constants q_u and q_d characterizing the supporting hyperplanes are easily calculated as:

$$q_u = c^T\pi + \left\|H^T c\right\|_1 \tag{26}$$

$$q_d = c^T\pi - \left\|H^T c\right\|_1 \tag{27}$$

where $\|.\|_1$ is the 1-norm of a vector. Then the intersection check is very easy to perform considering that each new measurement defines a set of consistent states defined by

$$F_k = \{x_k \in \Re^n : -\sigma \leq y_k - Cx_k \leq \sigma\} \tag{28}$$

where F_k is the region between two hyperplanes and the output y_k is considered component-wise. The normalized form of this strip is written as

$$\bar{F}_k = \{x_k \in \Re^n : |\frac{y_k}{\sigma} - c^T x_k| \leq 1\} \tag{29}$$

Calculating the supporting hyperplane constant q_u and q_d the intersection is empty if and only if:

$$q_u < \frac{y_k}{\sigma} - 1 \;\text{ or }\; q_d > \frac{y_k}{\sigma} + 1 \tag{30}$$

This condition of inconsistency for a SISO model was reported in Vicino and Zappa (1996).

5. CASE STUDY

5.1 Description of Twin-Rotor MIMO System

The twin-rotor MIMO system (TRMS) is a laboratory setup developed by Feedback Instruments Limited for control experiments. The system is perceived as a challenging engineering problem due to its high non-linearity, cross-coupling between its two axes, and inaccessibility of some of its states through measurements. The TRMS mechanical unit has two rotors placed on a beam together with a counterbalance whose arm with a weight at its end is fixed to the beam at the pivot and it determines a stable equilibrium position (Fig. 2). The TRMS consists of a beam pivoted on its base in such a way that it can rotate freely both in the horizontal and vertical planes. At both ends of the beam there are rotors (the main and tail rotors) driven by DC motors.

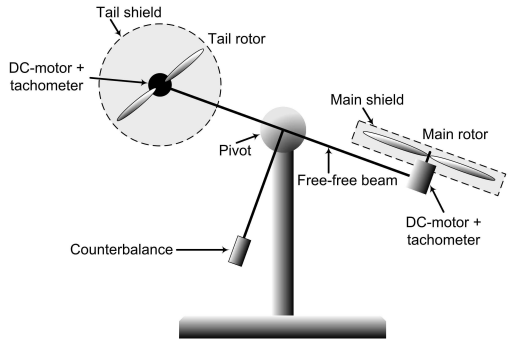

Figure 2. Components of the Twin Rotor MIMO System

The system input vector is $u = [u_t, \; u_m]^T$ where u_t is the input voltage of the tail motor and u_m is the input voltage of the main motor. On the other hand, the system states are $x = [\theta_h, \; \Omega_h, \; \omega_t, \; \theta_v, \; \Omega_v, \; \omega_m]^T$ where Ω_h is the angular velocity around the vertical axis, θ_h is the azimuth angle of beam (horizontal plane), ω_t is the rotational velocity of the tail rotor, Ω_v is the angular velocity around the horizontal axis, θ_v is the pitch angle of beam (vertical plane) and ω_m is the rotational velocity of the main rotor.

5.2 Non linear Model of Twin-Rotor MIMO System

The mathematical model is developed assuming that the dynamics of the propeller subsystem can be described by first order differential equations. Further, it is assumed that friction in the system is of the viscous type. Thus, the mathematical model of the TRMS becomes a set of the following nonlinear differential equations (Fee (1998)):

$$
\begin{aligned}
\dot{\theta}_h &= \Omega_h = S_h + \frac{J_{mr}\omega_m cos\theta_v}{J_h} \\
\dot{S}_h &= \frac{l_t F_h(\omega_t) cos\theta_v - \Omega_h k_h}{J_h} \\
\dot{\theta}_v &= \Omega_v = S_v + \frac{J_{tr}\omega_t}{J_v} \\
\dot{S}_v &= \frac{l_m F_v(w_m) + g((a-b)cos\theta_v - csin\theta_v)}{J_v} \\
&\quad - \frac{\Omega_v k_v - 0.5\Omega_h^2(a+b+c)sin2\theta_v}{J_v}
\end{aligned} \tag{31}
$$

where Ω_v and Ω_h are the angular velocities around the horizontal and the vertical axis, respectively. S_v and S_h are the angular momentum in vertical and horizontal plane of the beam, respectively. $F_v(\omega_m)$ and $F_h(\omega_t)$ are the dependence of the propulsive force on DC-motor rotational speeds:

$$
\begin{aligned}
F_v(\omega_m) &= -3\cdot 10^{-14}\omega_t^5 - 1.595\cdot 10^{-11}\omega_t^4 + 2.511\cdot 10^{-7}\omega_t^3 \\
&\quad -1.808\cdot 10^{-4}\omega_t^2 + 0.0801\omega_t \\
F_h(\omega_t) &= -3.48\cdot 10^{-12}\omega_m^5 + 1.09\cdot 10^{-9}\omega_m^4 + 4.123\cdot 10^{-6}\omega_m^3 \\
&\quad -1.632\cdot 10^{-4}\omega_m^2 + 9.544\cdot 10^{-2}\omega_m
\end{aligned}
$$

J_{tr} and J_{mr} are the moments of inertia in DC-motor tail and main propeller subsystem, respectively. The moment of inertia relative to vertical axis is $J_v = 0.055846$ and horizontal axis is:

$$J_h = dsin^2\theta_v + ecos^2\theta_v + f$$

$$
\begin{aligned}
a &= \left(\frac{m_t}{2} + m_{tr} + m_{ts}\right) l_t, \\
b &= \left(\frac{m_m}{2} + m_{mr} + m_{ms}\right) l_m, \\
c &= \frac{m_b}{2} l_b + m_{cb} l_{cb}, \\
e &= (\frac{m_m}{3} + m_{mr} + m_{ms}) l_m^2 + (\frac{m_t}{3} + m_{tr} + m_{ts}) l_t^2 \\
d &= \frac{m_b}{3} l_b^2 + m_{cb} l_{cb}^2 \\
f &= m_{ms} r_{ms}^2 + \frac{m_{ts}}{2} r_{ts}^2
\end{aligned}
$$

where m_{ms} and m_{ts} are the masses of the main and tail shields. m_m and m_t are the masses of the main and the tail parts of the beam, respectively. m_{mr} and m_{tr} are the masses of the main and the tail DC-motor with main and tail rotor,respectively. m_b and l_b are the mass and the length of the counter-weight beam. m_{cb} and l_{cb} represent the mass of the counter-weight and the distance between the counter-weight and the joint, respectively. r_{ms} and r_{ts} are the radius of the main and tail shield.

The rotational velocity of tail motor ω_t and the angular velocity of the main rotor ω_m are non linear functions of the input voltage of the DC-motor: $\omega_t = P_h(u_{hh})$ and $\omega_m = P_v(u_{vv})$ with

$$
\begin{aligned}
\dot{u}_{hh} &= \frac{1}{T_{tr}}(-u_{hh} + u_m) \\
\dot{u}_{vv} &= \frac{1}{T_{mr}}(-u_{vv} + u_t)
\end{aligned} \tag{32}
$$

T_{mr} and T_{tr} are the time constant of main and tail motor-propeller system, respectively.

5.3 The TRMS LPV model and observer design

There are different ways to obtain LPV models. Some methods use the nonlinear equations of the system to derive LPV model such as state transformation, function substitution and methods using Jacobian linearization (Shamma and Cloutier, 1993). Other methods use multi-model identification that consists in two-step procedure. First LTI models are identified at different equilibrium points by classical methods, then a global multi-model is obtained by interpolating among the local LTI models (Murray-Smith and Johansen, 1997, Baranyi et al., 2003). The multiple model approach obtained by physical laws or identification can be viewed as a single linear parameter varying (LPV) global model. Another technique is the LPV identification that represents an extension of the classical identification (linear regression, subspace) methods (Bamieh and Giarré, 2002).

In this case, the multiple linear model identification is used around five different points (see Table 1) with a sampling time $T_s = 0.025s$. The system has been identified using the input $u = [u_t, u_m]^T$ and the output $y = [\theta_h, \theta_v]^T$. Then the discrete state space (7) is composed of the following matrices:

$$
A_1 = \begin{bmatrix}
1 & 0.025 & 0 & 0 & 0 & 0.0142 \\
0 & 0.9905 & 0 & 0 & 0.0995 & -0.0054 \\
0 & 0 & 1 & 0.025 & 0.0732 & 0 \\
0 & 0 & -0.0862 & 0.9976 & -0.0071 & 0.0078 \\
0 & 0 & 0 & 0 & 0.9349 & 0 \\
0 & 0 & 0 & 0 & 0 & 0.9825
\end{bmatrix},
$$

$$
A_2 = \begin{bmatrix}
1 & 0.025 & -0.0005 & 0 & 0 & 0.0141 \\
0 & 0.9906 & 0.0002 & 0 & 0.0991 & -0.0053 \\
0 & 0 & 1 & 0.025 & 0.0732 & 0 \\
0 & 0 & -0.0862 & 0.9976 & -0.0071 & 0.0102 \\
0 & 0 & 0 & 0 & 0.9349 & 0 \\
0 & 0 & 0 & 0 & 0 & 0.9825
\end{bmatrix},
$$

$$
A_3 = \begin{bmatrix}
1 & 0.025 & -0.0010 & 0 & 0 & 0.0137 \\
0 & 0.9908 & 0.0004 & 0 & 0.0985 & -0.0050 \\
0 & 0 & 1 & 0.025 & 0.0732 & 0 \\
0 & 0 & -0.0862 & 0.9976 & -0.0071 & 0.0207 \\
0 & 0 & 0 & 0 & 0.9349 & 0 \\
0 & 0 & 0 & 0 & 0 & 0.9825
\end{bmatrix},
$$

$$
A_4 = \begin{bmatrix}
1 & 0.025 & -0.0015 & 0 & 0 & 0.0131 \\
0 & 0.9912 & 0.0005 & 0 & 0.0973 & -0.0046 \\
0 & 0 & 1 & 0.025 & 0.0732 & 0 \\
0 & 0 & -0.0862 & 0.9976 & -0.0071 & 0.0375 \\
0 & 0 & 0 & 0 & 0.9349 & 0 \\
0 & 0 & 0 & 0 & 0 & 0.9825
\end{bmatrix},
$$

$$
A_5 = \begin{bmatrix}
1 & 0.025 & -0.0020 & 0 & 0 & 0.0123 \\
0 & 0.9918 & 0.0006 & 0 & 0.0953 & -0.0040 \\
0 & 0 & 1 & 0.025 & 0.0732 & 0 \\
0 & 0 & -0.0860 & 0.9976 & -0.0071 & 0.0575 \\
0 & 0 & 0 & 0 & 0.9349 & 0 \\
0 & 0 & 0 & 0 & 0 & 0.9825
\end{bmatrix},
$$

$$
B = \begin{bmatrix} 0 & 0 & 0 & 0 & 0.025 & 0 \\ 0 & 0 & 0 & 0 & 0 & 0.025 \end{bmatrix}^T,
$$

$$
C = \begin{bmatrix} 1 & 0 & 0 & 0 & 0 & 0 \\ 0 & 0 & 1 & 0 & 0 & 0 \end{bmatrix},
$$

where the scheduling variable is the azimuth angle of beam θ_h and $\alpha^j(p_k)$ can be determined from (6).

N	$\overline{u}_t$	$\overline{u}_m$	$\overline{\theta}_h$	$\overline{\theta}_v$
1	0	0	0	-0.9326
2	0	0.05	0.1074	-0.9257
3	0	0.10	0.2146	-0.9133
4	0	0.15	0.3199	-0.8895
5	0	0.20	0.4211	-0.8501

Table 1. Equilibrium points of the each j^{th} linear model.

The LTI systems are incremental and the equilibrium conditions of Table 1 should be added. Consequently, the expressions of these conditions are:

$$\hat{y}(k) = \sum_{j=1}^{N} \alpha^j(\vartheta_k) \left[C_j \hat{x}(k) + \overline{y}_j \right] \tag{33}$$

where $\overline{y}_j = [\overline{\theta}_h^j,\ \overline{\theta}_v^j]^T$ (See Table 1).

Additionally, uncertainty has been included in some parameters of the observer model to take into account the difference between the LPV model and the real nonlinear behavior: $a_{22}^j \in [a_{22}^j \pm 0.0092]$, $a_{43}^j \in [a_{43}^j \pm 0.0133]$ and $a_{46}^j \in [a_{46}^j \pm 0.0107]$ for $j = 1, \ldots, N$. This uncertainty will be taken into account when generating the set of output behaviors using the interval LPV observer (7).

The proposed observer design procedure was applied to obtain L_j such that the poles are in disk LMI region with the parameters $c = -0.5$ and $r = 0.5$. In the design of the observer gains L_j uncertainty in matrix $A_j(\vartheta^j)$ has been considered.

Fig. 3 presents the time evolution responses of outputs and their adaptive thresholds in different operating points. Fig. 3(b) shows the pitch angle of beam and Fig. 3(c) presents its residual response. It can be seen that the adaptive threshold changes in the system dynamics.

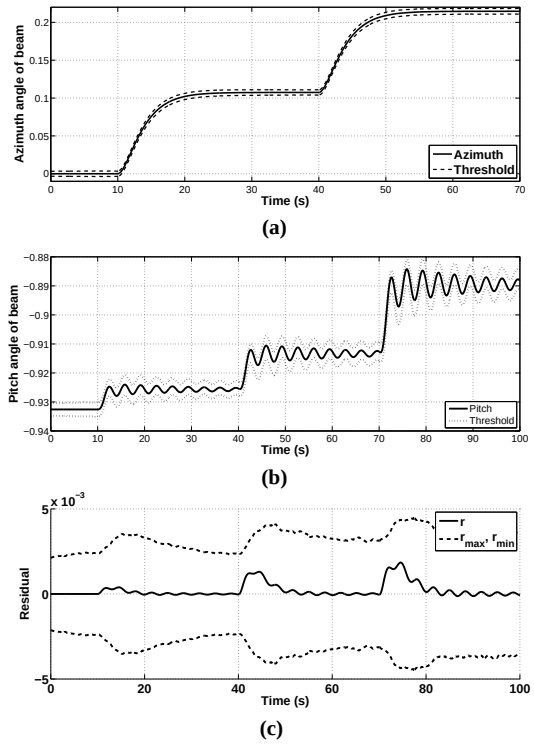

Figure 3. (a) Azimuth angle of beam. (b) Pitch angle of beam. (c) Residual of pitch angle of beam

5.4 Fault scenarios

The fault scenarios were implemented in nonlinear TRMS equations (31)-(32) using interval LPV observer designed in the previous section. Figs. (4)-(5) present the results and the fault detection indicator is presented at the bottom of each graph.

5.4.1 Fault scenario 1. An additive actuator fault of the tail motor f_{a_t} is defined as:

$$f_{a_t}(t) = \begin{cases} 0, & \text{for} \quad t < 40 \\ 0.025, & \text{for} \quad t \geq 40 \end{cases} \tag{34}$$

Fig. 4(a) shows the azimuth angle of beam θ_h and its adaptive threshold. The prediction bounds of the azimuth angle of beam θ_h are obtained using zonotopes (see Section 4) and taking into account the uncertainty in the parameters. Fig. 4(b) shows the residual signal for azimuth angle of beam θ_h and the envelopes computed using the zonotope method. The envelopes of the residual are adapted following the changes in the system dynamics. The fault detection test in both cases shows that the fault alarm is activated in $t = 41.5s$ and the alarm keeps constant until $t = 44.6s$.

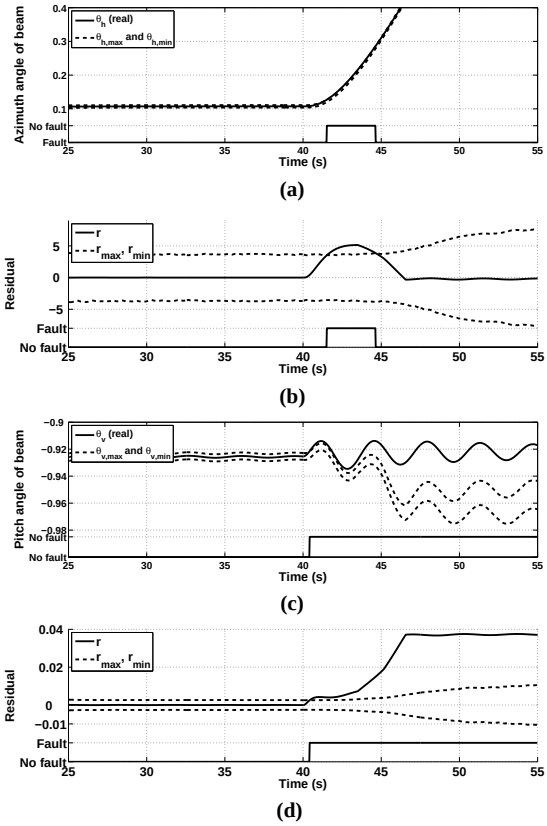

Figure 4. (a) Azimuth angle of beam in presence of fault f_{a_t}. (b) Residual of azimuth angle of beam in presence of fault f_{a_t} (c) Pitch angle of beam in presence of fault f_{a_t}. (d) Residual of pitch angle of beam in presence of fault f_{a_t}

Fig. 4(c) shows the pitch angle of beam θ_v and its adaptive threshold. The bounds of pitch angle of beam θ_v are obtained using the zonotope algorithm. Fig. 4(d) presents its residual response and its adaptive threshold. In this case, the fault detection test shows that the fault alarm is activated in $t = 40.4s$.

5.4.2 Fault scenario 2. An additive sensor fault of the pitch angle of beam f_{θ_v} is defined as:

$$f_{\theta_v}(t) = \begin{cases} 0, & \text{for} \quad t < 40 \\ 0.015, & \text{for} \quad t \geq 40 \end{cases} \tag{35}$$

Fig. 5(a) shows the azimuth angle of beam θ_h and its adaptive threshold. The fault detection test (20) detects the fault in the time $t = 42.9s$. Fig. 5(b) shows the residual signal for azimuth angle of beam θ_h and its envelopes that are based on zonotope algorithm.

Finally, Fig. 5(c) shows the pitch angle of beam θ_v and its adaptive threshold. Fig. 5(d) shows the residual signal for pitch angle of beam θ_v and the envelopes computed using the zonotope

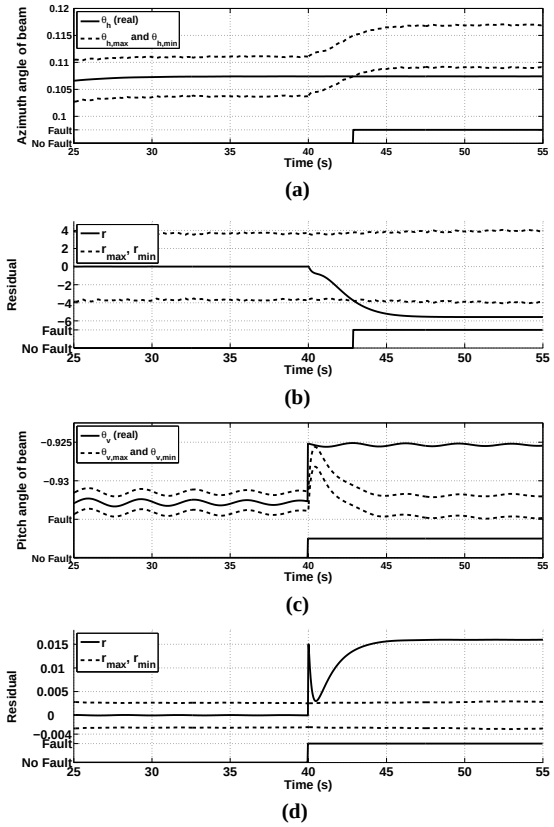

Figure 5. (a) Azimuth angle of beam in presence of fault f_{θ_v}. (b) Residual of azimuth angle of beam in presence of fault f_{θ_v} (c) Pitch angle of beam in presence of fault f_{θ_v}. (d) Residual of pitch angle of beam in presence of fault f_{θ_v}

method. The envelopes of the residual are adapted following the changes in the system dynamics. The fault detection test in both cases shows that the fault alarm is activated in $t = 40.025s$.

6. CONCLUSIONS

In this paper, a robust fault detection using interval LPV observer using zonotopes has been proposed. The gain of the interval LPV observer has been designed using LMI formulation. This method guarantees the pole placement of the observer for each vertex with uncertainties. As a result a set of gains is obtained and these are interpolated to calculate the gain of interval LPV observer (7). A set of estimated outputs based on propagating the uncertainty using zonotopes is proposed. This set has been used to implement the fault detection test. Finally, a TRMS has been used as a case study. It has been described by means of LPV model with uncertainties, which were considered unknown but bounded by intervals. According to the results obtained in the considered fault scenarios, the proposed fault detection approach has been successfully applied.

7. ACKNOWLEDGMENTS

This work has been partially funded by the grant CICYT DPI2008-01996 of Spanish Ministry of Education, the by Research Comission of the Generalitat de Catalunya (group SAC ref. 2005SGR00537) and by a grant from Consejo Nacional de Ciencia y Tecnologia de México (CONACyT).

REFERENCES

T. Alamo, J.M. Bravo, and E.F. Camacho. Guaranteed state estimation by zonotopes. *Automatica*, 41(6):1035–1043, 2005.

M. Andrés and G. J. Balas. Development of linear-parameter-varying models for aircraft. *Journal of Guidance, Control and Dynamics*, 27(2):218–228, 2004.

P. Apkarian, P. Gahinet, and G. Becker. Self-scheduled H_∞ control of linear parameter-varying systems: a design example. *Automatica*, 31(9):1251 – 1261, 1995.

B. Bamieh and L. Giarré. Identification of linear parameter varying models. *International Journal Robust Nonlinear Control*, 2(12):841–853, 2002.

P. Baranyi, D. Tikk, Y. Yam, and R. J. Patton. From differential equations to PDC controller design via numerical transformation. *Computers in Industry, Elsevier Science*, 51:281–297, 2003.

J. Bokor, Z. Szabo, and G. Stikkel. Failure detection for quasi LPV systems. *Proceedings of the 41st IEEE Conference on Decision and Control*, 3:3318–3323, 2002.

J. Chen and R. J. Patton. *Robust model-based fault diagnosis for dynamic systems*. Kluwer Academic Publishers, 1999.

M. Chilali and P. Gahinet. H_∞ design with pole placement constraints: an LMI approach. *IEEE Transactions on Automatic Control*, 41(3):358–367, 1996.

C. Combastel. A state bounding observer based on zonotopes. In *European Control Conference*, 2003.

Twin Rotor MIMO System Advanced Teaching Manual 1 (33-007-4M5). Feedback Instruments Ltd, Crowborough, UK., 1998.

D. T. Horak. Failure detection in dynamic systems with modelling errors. *Journal of Guidance, Control, and Dynamics*, 11(6):508–516, 1988.

W. Kuhn. Rigorously computed orbits of dynamical systems without the wrapping effect. *Computing*, 61(1):47–67, 1998.

D. Maksarov and J.P. Norton. State bounding with ellipsoidal set description of the uncertainty. *International Journal of Control*, 65 (5):847 – 866, 1996.

M. Milanese, J. Norton, H. Piet-Lahanier, and É. Walter, editors. *Bounding Approaches to System Identification*. Springer, 1996.

R.E. Moore. *Interval analysis*. Prentice Hall, 1966.

R. Murray-Smith and T. A. Johansen. *Multiple Model Approaches to Modelling and Control*. Taylor and Francis, 1997. ISBN 0-7484-0595-X.

V. Puig, J. Quevedo, and T. Escobet. Robust fault detection approaches using interval models. In *IFAC World Congress (b'00)*, Barcelona, Spain, 2002.

B. Rinner and U. U. Weiss. Online monitoring by dynamically refining imprecise models. *IEEE Transactions on Systems, Man and Cybernetics: Part B*, 34 (4):1811 – 1822, 2004.

J.S. Shamma and J.R. Cloutier. Gain scheduled missile autopilot design using linear parameter varying transformations. *AIAA Journal of Guidance, Control, and Dynamics*, 16(2): 256–263, 1993.

A. Vicino and G. Zappa. Sequential approximation of feasible parameter sets for identification with set membership uncertainty. *IEEE Transactions on Automatic Control*, 41:774–785, 1996.

M. Witczak, J. Korbicz, and R.J. Patton. A bounder-error approach to designing unknown input observers. In *IFAC World Congress (b'02)*, Barcelona, Spain, 2002.